

## **MEMS for structural health monitoring of wind turbine blades**

Aubryn M. Cooperman, Marcias J. Martinez

Faculty of Aerospace Engineering, Delft University of Technology, Kluyverweg 1, P.O. Box 5058, 2600 GB Delft, The Netherlands

### **Abstract**

Structural health monitoring is becoming more valuable for wind energy producers as wind farms become larger and more remote. Increasing numbers of wind turbines are being installed offshore in order to take advantage of the higher wind speeds and more consistent wind resource available over the water. High winds and waves make access to offshore wind farms more limited than at onshore sites, making early identification and monitoring of developing repair and maintenance needs much more important. As structural health monitoring becomes a priority for offshore turbines, there is a need for appropriate sensors for this task. The rotor blades are a key location to monitor, as they are responsible for all of the energy capture of the turbine. Rotor blades are also among the top contributors to unplanned downtime, alongside the gearbox and generator. Improved structural health monitoring of the blades therefore has the potential to provide significant benefits. The proposed sensor system for wind turbine rotor blades is based on micro-electromechanical systems (MEMS) incorporating tri-axial gyroscopes, accelerometers and magnetometers. The MEMS, distributed along the blade, enable precise determination of the orientation of each blade segment. Orientation information from each MEMS is used to find the deformation shape of the blade, which is the input to a finite element model for calculation of the strains and stresses over the entire blade. As an initial test of the system, the MEMS are affixed to a beam under a static bending load. The output from each accelerometer, gyroscope and magnetometer is combined and filtered to produce an estimate of the local deflection angles. Information from several sensors is used to determine the beam deformation. Finite element analysis of the deformation will produce a strain distribution for the entire beam, which can be compared with strain measured at various points on the beam using conventional strain gauges.

### **1. INTRODUCTION**

Wind turbine blades operate in a dynamic environment where they are subjected to constantly changing load conditions. Understanding the structural health of the blades is critical for ensuring safe operation of a wind turbine and anticipating maintenance needs. Various methods of assessing the structural health of wind turbine blades have been proposed and implemented, including fiber optic strain gauges, ultrasonic testing and acoustic emission<sup>1</sup>. Inertial sensors based on micro-electromechanical systems (MEMS) have been tested for aerospace applications<sup>2</sup> and have the potential to provide valuable information for the structural health monitoring of wind turbines as well.

MEMS sensors can be used to detect blade deformation including flapwise and edgewise bending as well as twist. In combination with a structural model, this deformation information can be used to determine stress and strain values throughout the blade. A long-term goal is for blade deformation measurements, in combination with other measurements on a turbine, to contribute to a holistic structural integrity process that enables prognostic asset management.

## 2. METHODS

A multi-sensor approach based on micro-electromechanical systems is used to analyze deformation of a beam. MEMS are manufactured using integrated circuit fabrication techniques and combine mechanical and electrical components on a scale of microns to millimeters. The sensors are manufactured by Motion Workshop<sup>3</sup>. A complete sensor package includes triaxial accelerometers, gyroscopes and magnetometers, as well as a thermocouple for temperature compensation, all incorporated into a single unit with dimensions of approximately  $35 \times 35 \times 15$  mm and a weight of 10 grams. Data is recorded at a rate of 100 Hz. The MEMS are available as wireless sensors or using wired USB connections. The small size, light weight and comparatively low cost of MEMS devices allows for the installation of a network of sensors within a structure. Compared to bulk devices, however, MEMS inertial sensors suffer from higher levels of noise and bias and offer lower precision. To address these shortcomings, a filtering algorithm has been applied to the MEMS sensors using the extended Kalman filter and combining the output of magnetometers, accelerometers and gyroscopes into a single value. Fusion of the inertial and magnetic sensor outputs provides more accurate estimation of the sensor orientation than would be achieved using a single measurement.

**Table 1** Sensor specifications<sup>3</sup>

Sensor	Range	Resolution
Accelerometer	$\pm 2 g$	200 $\mu g$
Magnetometer	$\pm 100 \mu T$	0.1 $\mu T$
Gyroscope	$\pm 2000 \text{ }^\circ/s$	0.07 $^\circ/s$

### 2.1 Sensor orientation

Orientation data from the MEMS sensors is expressed mathematically using quaternions. Quaternions are as useful means of computing orientations for various types of aerospace applications<sup>4</sup>. A quaternion has four parts: a scalar part and three orthogonal vector components:

$$q = q_0 + \mathbf{i}q_1 + \mathbf{j}q_2 + \mathbf{k}q_3$$

where  $\mathbf{i}$ ,  $\mathbf{j}$  and  $\mathbf{k}$  are the orthogonal basis vectors associated with the  $x$ ,  $y$  and  $z$  axes, respectively, and  $q_0$ ,  $q_1$ ,  $q_2$  and  $q_3$  are scalars. The quaternion representation is advantageous because it has smooth continuous behavior throughout the domain (no singular points). Quaternions can be used to evaluate a change in orientation without requiring knowledge of the initial position vector. They can also be used to evaluate the relative orientations of two or more objects.

Quaternions representing the orientation of each sensor are determined using output from the accelerometers and magnetometers. Accelerometers detect the angle of the sensor with respect to the gravity vector that defines the vertical direction, while magnetometers detect the sensor's orientation with respect to the Earth's magnetic field. The magnetic field vector provides a reference to orient the sensor in the horizontal plane. The acceleration and magnetic field measurements are combined using a factored quaternion algorithm (FQA)<sup>5</sup>. Magnetometers are sensitive to electromagnetic interference from sources other than the Earth's magnetic field, such as nearby ferromagnetic materials or electronics. The FQA minimizes the impact of magnetic interference by calculating the sensor pitch and roll angles using solely the accelerometer output. The magnetometer output is used only to determine the azimuth angle. Pitch, roll and azimuth are expressed in a quaternion representation to avoid singular behavior in the polar directions.

The third component of the sensor package is a gyroscope, which provides information on the angular rate,  $\omega_i$ , about each axis. The angular rates are incorporated into estimates of the sensor orientation via a Kalman filter. Various types of Kalman filter are used to estimate the state of dynamic systems; for this system, an extended Kalman filter (EKF) formulation was chosen. The EKF is the most common choice of Kalman filter for nonlinear processes<sup>6</sup>, and can be implemented relatively simply. The error between the true state of the system and the estimated state is represented by a linearized first-order Taylor series expansion. In applying the extended Kalman filter to inertial and magnetic sensors, we follow the approach of Yun and Bachmann<sup>7</sup>. The state vector  $x$  is:

$$x = \begin{bmatrix} \omega_1 \\ \omega_2 \\ \omega_3 \\ q_0 \\ q_1 \\ q_2 \\ q_3 \end{bmatrix}$$

with the state updates given by:

$$\begin{bmatrix} \dot{\omega}_1 \\ \dot{\omega}_2 \\ \dot{\omega}_3 \end{bmatrix} = \frac{1}{\tau} \left( - \begin{bmatrix} x_1 \\ x_2 \\ x_3 \end{bmatrix} + \begin{bmatrix} \omega_1 \\ \omega_2 \\ \omega_3 \end{bmatrix} \right) \text{ and } \begin{bmatrix} \dot{q}_0 \\ \dot{q}_1 \\ \dot{q}_2 \\ \dot{q}_3 \end{bmatrix} = \frac{1}{2} \begin{bmatrix} q_0 \\ q_1 \\ q_2 \\ q_3 \end{bmatrix} \otimes \begin{bmatrix} 0 \\ \omega_1 \\ \omega_2 \\ \omega_3 \end{bmatrix}$$

where  $\dot{\omega}_i, \dot{q}_i$  are time derivatives,  $\tau$  is a time constant and  $\otimes$  denotes quaternion multiplication. The measurement vector  $z$  consists of the same quantities as the state vector: the measured angular rates and the orientation quaternion produced by the FQA from the magnetometer and accelerometer measurements. The structure of the resulting algorithm is shown schematically in Figure 1.

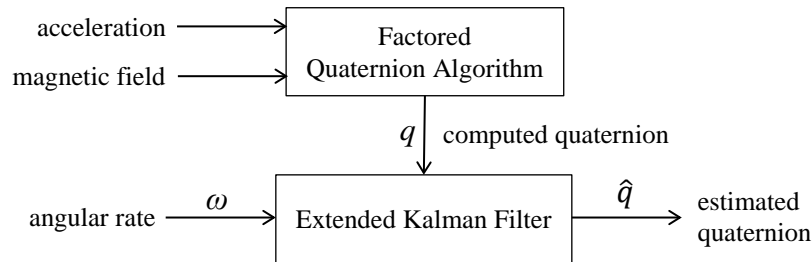


**Figure 1.** Kalman filter design<sup>7</sup>

For evaluation of structural deformation, the key information is the relative orientation of each sensor, not its absolute orientation. The estimated quaternions for each sensor are normalized based on the fixed reference sensor at the beam root, using the equation

$$q_{rel} = \hat{q} \otimes \hat{q}_{ref}^{-1}$$

where the subscripts *rel* and *ref* describe the relative orientation and reference quaternions.

## 2.2 Test setup

The platform used to demonstrate this methodology for determining deformation is a cantilever beam instrumented with 5 MEMS sensors and 4 foil strain gauges, which is subjected to axial bending with a maximum tip deflection of 5.8 cm (Figure 2). A sixth MEMS sensor is fixed to the rigid test frame to act as a reference signal for the five sensors on the beam. The aluminum beam has a constant rectangular cross section with a width of 60 mm and a height of 5.2 mm. The distance from the clamp to the point at the tip where the displacement is introduced is 80 cm. The strain gauges and MEMS sensors are located at equally-spaced intervals of 9 cm along the central axis of the beam.

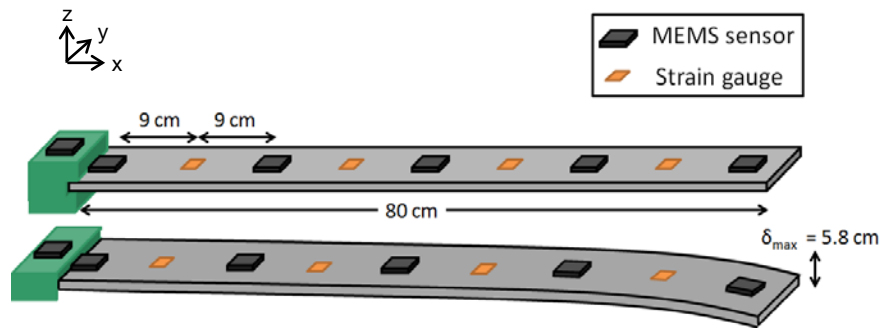


Figure 2. Cantilever beam layout

## 2.3 Shape estimation

The normalized quaternions are used to determine the beam deformation, based on a cantilever beam shape estimation algorithm developed by Kirby *et al*<sup>8</sup>. The angle of each sensor with respect to the beam axis describes the local slope at the sensor location. An overall beam deformation can be estimated by integrating the slope at each point. The deformation shape is assumed to take the form of a cubic polynomial, consistent with Euler-Bernoulli beam theory. The beam is divided into two segments comprising three sensor nodes, with the center node appearing in both segments. The coefficients of the cubic polynomial for each section is determined using a least-squares fit with the constraints that the slope and displacement must be equal at the intersection of the segments, and zero at the clamped end.

### 3. RESULTS

Deformation shapes obtained using the MEMS sensors are shown in Figure 3, where they are compared to the expected deformation shapes based on Euler-Bernoulli beam theory. For maximum displacements above 30 mm, or 3.8% of the beam length, there is good agreement between the theoretical and estimated tip displacements, but the estimated beam shapes show greater curvature in the outer half of the beam. For smaller maximum displacements, small deviations in the estimated sensor orientations lead to larger variations in the total estimated deformation. This is most evident in the neutral beam (0 mm tip displacement).

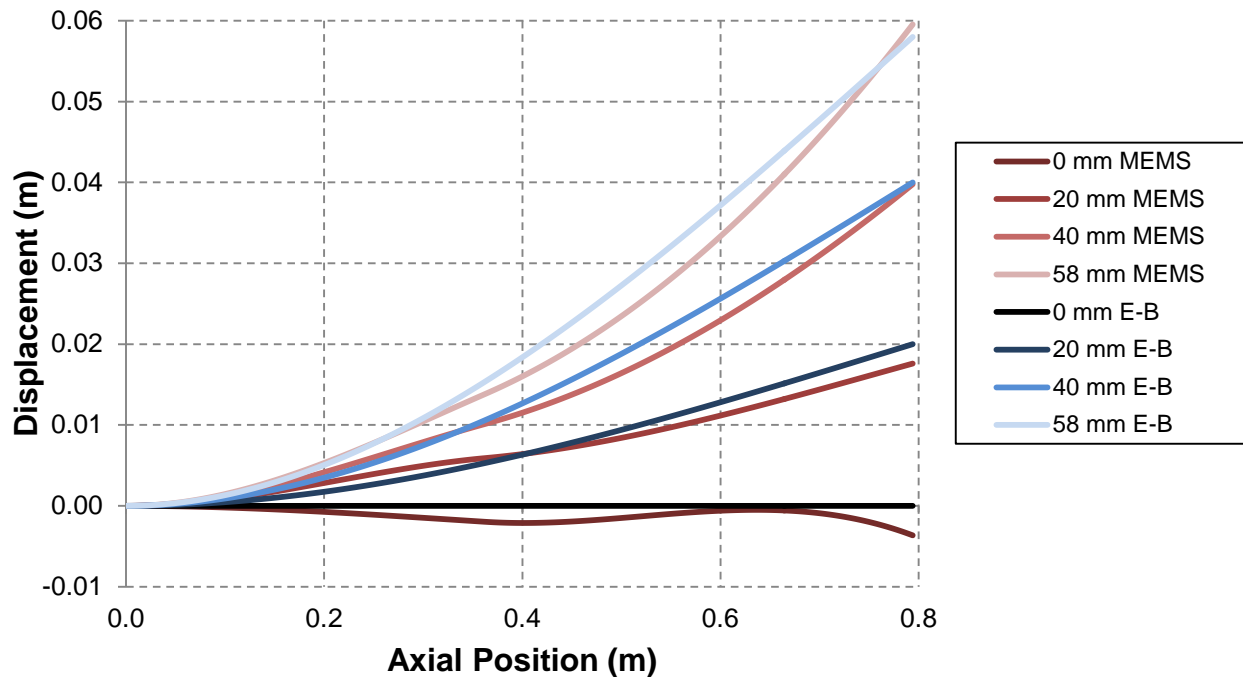


**Figure 3.** Comparison of estimated beam shapes based on MEMS orientation sensors with Euler-Bernoulli beam theory (E-B). Legend entries for each curve indicate the tip displacement.

### 4. CONCLUSIONS AND FUTURE WORK

In order to develop a complete understanding of the beam structure, the estimated beam deflections will be input to a finite element model (FEM) as an initial displacement. From the FEM, stress and strain can be calculated at any point within the structure. Comparison of the strain gauge measurements with the FEM results will allow for evaluation of the accuracy of the MEMS sensor methodology for deformation measurements on a cantilever beam.

In the future, this methodology will be tested on a more complex structure, a composite blade designed for a small wind turbine. The 1.7 m diameter WindChallenge turbine is intended for rooftop installation and will provide a rotating test environment for the MEMS sensors.

## ACKNOWLEDGMENTS

The contributions of Matthew Li and Bruno Rocha in developing the Kalman filter are very much appreciated. This research has been supported by the Dutch Ministry of Economic Affairs through the Far and Large Offshore Wind programme (FLOW) and by the FP7 Marie Curie Career Integration Grant titled Monitoring of Aerospace Structural Shapes (MASS).

## REFERENCES

1. García Márquez, F. P., Tobias, A. M., Pinar Pérez, J. M., and Papaalias, M. "Condition monitoring of wind turbines: Techniques and methods," *Renewable Energy*, Vol. 46, Oct. 2012, pp. 169–178.
2. Martinez, M., Rocha, B., Li, M., Shi, G., Beltempo, A., Rutledge, R., and Yanishevsky, M. "Load monitoring of aerospace structures utilizing micro-electro-mechanical systems for static and quasi-static loading conditions," *Smart Materials and Structures*, Vol. 21, No. 11, 2012, pp. 115001-11.
3. Motion Workshop. <http://www.motionnode.com/>
4. Kuipers, J.B. *Quaternions and rotation sequences: a primer with applications to orbits, aerospace, and virtual reality*. Princeton University Press: Princeton, NJ, 1999.
5. Yun, X., Bachmann, E. R., and McGhee, R. B. "A Simplified Quaternion-Based Algorithm for Orientation Estimation From Earth Gravity and Magnetic Field Measurements," *IEEE Transactions on Instrumentation and Measurement*, Vol. 57, No. 3, Mar. 2008, pp. 638–650.
6. Crassidis, J. L. and Junkins, J. L. *Optimal estimation of dynamic systems*. Boca Raton: Chapman & Hall/CRC, 2004.
7. Yun, X., and Bachmann, E. R. "Design, Implementation, and Experimental Results of a Quaternion-Based Kalman Filter for Human Body Motion Tracking," *IEEE Transactions on Robotics*, Vol. 22, No. 6, 2006, pp. 1216–1227.
8. Kirby, G. C., Lim, T. W., Weber, R., Bosse, A., Povich, C., and Fisher S. "Strain-based shape estimation algorithms for a cantilever beam," *SPIE Proceedings*, Vol. 3041, 1997, pp. 788–798.